

Suppression of the metal-insulator transition by magnetic field in $(\text{Pr}_{1-y}\text{Y}_y)_{0.7}\text{Ca}_{0.3}\text{CoO}_3$ ($y = 0.0625$)

Tomoyuki Naito,^{1,a)} Hiroyuki Fujishiro,¹ Terukazu Nishizaki,² Norio Kobayashi,² Jiří Hejtmánek,³ Karel Knížek,³ and Zdeněk Jirák³

¹Faculty of Engineering, Iwate University, Morioka 020-8551, Japan

²Institute for Materials Research, Tohoku University, Sendai 980-8577, Japan

³Institute of Physics, ASCR, Cukrovarnická 10, 162 00 Prague 6, Czech Republic

(Received 20 February 2014; accepted 2 June 2014; published online 19 June 2014)

The $(\text{Pr}_{1-y}\text{Y}_y)_{0.7}\text{Ca}_{0.3}\text{CoO}_3$ compound ($y = 0.0625$, $T_{\text{MI-SS}} = 40$ K), at the lower limit for occurrence of the first-order metal-insulator (MI) and simultaneous spin-state (SS) transitions, has been studied using electrical resistivity and magnetization measurements in magnetic fields up to 17 T. The isothermal experiments demonstrate that the low-temperature insulating phase can be destabilized by an applied field and the metallic phase returns well below the transition temperature $T_{\text{MI-SS}}$. The reverse process with decreasing field occurs with a significant hysteresis. The temperature scans taken at fixed magnetic fields reveal a parabolic-like decrease in $T_{\text{MI-SS}}$ with increasing field strength and a complete suppression of the MI-SS transition in fields above 9 T.

© 2014 AIP Publishing LLC. [<http://dx.doi.org/10.1063/1.4884435>]

I. INTRODUCTION

The Co^{3+} ions in the LaCoO_3 cobaltite and its rare-earth analogs have been extensively studied for the past five decades as controversy still remains over whether their spin-state (SS) transition occurs between the low-spin (LS) state ($t_{2g}^6 e_g^0$, $S = 0$) and the intermediate-spin (IS) state ($t_{2g}^5 e_g^1$, $S = 1$) or high-spin (HS) state ($t_{2g}^4 e_g^2$, $S = 2$).^{1,2} Still lesser understanding concerns the nature of the ferromagnetic metallic phase in mixed-valence cobaltites of the $\text{La}_{1-x}\text{Sr}_x\text{CoO}_3$ type. It is argued that localized models cannot describe appropriately all the cobaltite complexity since the Co e_g states interact with O $2p$ states and are spread over a large energy range.³ More recent dynamic mean field theory (DMFT) calculations thus suggest for $\text{La}_{1-x}\text{Sr}_x\text{CoO}_3$ a complex global state that can be locally understood as a dynamic fluctuation over different cobalt valences and spin states,⁴ but with certain simplification, the metallic nature of these phases and their ferromagnetic ground state can be related to an electron transfer between neighbors of the $\text{IS-Co}^{3+}/\text{LS-Co}^{4+}$ or $\text{HS-Co}^{3+}/\text{HS-Co}^{4+}$ kinds, eventually also $\text{LS-Co}^{3+}/\text{LS-Co}^{4+}$.⁵

To account for the magnetic properties actually observed, in particular, the low-temperature spontaneous moments and effective moments at intermediate temperatures, one may conclude on a domination of the $\text{IS-Co}^{3+}/\text{LS-Co}^{4+}$ pairs in $\text{La}_{1-x}\text{Sr}_x\text{CoO}_3$.⁶ The situation is changed in systems in which the large La and Sr cations are substituted by smaller rare-earth and calcium cations. Still within the simplified model of localized states, these systems show on cooling a gradual spin-state crossover toward a $\text{LS-Co}^{3+}/\text{LS-Co}^{4+}$ mixture.⁷ A distinct behavior takes place in some Pr-based mixed-valence cobaltites, in which the crossover to lower spin states acquires a form of first-order transition of metal-insulator (MI) type. This transition was observed for the first time in oxygen stoichiometric $\text{Pr}_{0.5}\text{Ca}_{0.5}\text{CoO}_3$ and was reported as having a

pronounced peak in heat capacity and sharp changes in magnetic susceptibility, electrical resistivity, thermopower, and unit cell volume at $T_{\text{MI-SS}} \sim 90$ K.^{8,9} The same phenomenon was evidenced later for analogous systems with lower calcium content, provided that they were either subjected to high pressures (physical pressure)¹⁰ or the praseodymium sites were suitably doped by yttrium or smaller rare-earth cations like Sm, Gd, and Tb (chemical pressure).^{10,11} Some empirical rules for the appearance of the MI transition were derived with regard to the values of cationic radii at the perovskite A-sites and their variance (size mismatch).¹¹

It was found that the key to this specific MI-SS transition was a significant shift from mixed-valence $\text{Co}^{3+}/\text{Co}^{4+}$ ions to pure Co^{3+} ion, enabled by the simultaneous change in valence of some Pr^{3+} ions into Pr^{4+} ions. For the prototypical compound $\text{Pr}_{0.5}\text{Ca}_{0.5}\text{CoO}_3$ this valence shift was confirmed and determined quantitatively with the identification of the Pr^{4+} -related Schottky peak in heat capacity measurements¹² and by X-ray absorption spectroscopy at the Pr L_3 edge.¹³ Similar evidence was presented also for the $\text{Pr}_{0.7}\text{Ca}_{0.3}\text{CoO}_3$ systems doped by Y,¹⁴⁻¹⁶ Sm,¹⁷ and Tb.¹⁸ Many studies have been done especially on the $(\text{Pr}_{1-y}\text{Y}_y)_{0.7}\text{Ca}_{0.3}\text{CoO}_3$ system, which displays a MI-SS transition and partial $\text{Pr}^{3+} \rightarrow \text{Pr}^{4+}$ valence shift at critical temperatures increasing from $T_{\text{MI-SS}} = 40$ K for $y = 0.0625$ up to $T_{\text{MI-SS}} = 132$ K for the yttrium solubility limit $y = 0.15$. No valence shift and, therefore, no MI-SS transition have been observed for $y = 0$ and 0.05 under ambient pressure.

It is natural to suspect that the external magnetic field stabilizes the higher spin states and should thus influence the transition temperature. Magnetic control of the SS transition in a spin-crossover complex was attempted for several ferrous compounds. $\text{Fe}(\text{phen})_2(\text{NCS})_2$ (phen = *ortho*-phenanthroline) showed the spin-crossover between LS and HS states of ferrous ions at 176 K. The transition temperature decreased by only 0.11 ± 0.04 K as the magnetic field was increased from 1.0 to 5.5 T, demonstrating that the variation

^{a)}Electronic mail: tnaito@iwate-u.ac.jp

is slight.¹⁹ A small decrease in the spin-crossover temperature was found also in $[\text{Fe}(\text{2-pic})_3]\text{Cl}_2 \cdot \text{EtOH}$ (2-pic = 2-amino-methyl-pyridine), in which the spin-crossover temperature between LS- and HS- Fe^{2+} states was suppressed only by approximately 0.2 K at 7 T from 113 K.²⁰ Similar experiments performed so far on the present $(\text{Pr}_{1-y}\text{Y}_y)_{0.7}\text{Ca}_{0.3}\text{CoO}_3$ ($y = 0.075 - 0.15$) system showed a comparable variation with the magnetic field.²¹ In particular, $T_{\text{SS}} = T_{\text{MI}} = 64.0$ K, determined for the $y = 0.075$ sample from susceptibility measurements at 0.1 T, decreased by 0.35 K in a magnetic field of 7 T.

This paper focuses on the $y = 0.0625$ compound that exhibits pronounced thermal hysteresis during the transition, related most likely to its low critical temperature. The magnetic and electrical properties for high external fields up to 17 T are presented. In contrast to yttrium-rich members of the $(\text{Pr}_{1-y}\text{Y}_y)_{0.7}\text{Ca}_{0.3}\text{CoO}_3$ series, a significant shift in the critical temperature with applied field and a complete suppression of the MI-SS transition in fields of 9 T and higher, is observed.

II. EXPERIMENTAL PROCEDURE

The $(\text{Pr}_{1-y}\text{Y}_y)_{0.7}\text{Ca}_{0.3}\text{CoO}_3$ ($y = 0.0625$) compound was prepared by a solid-state reaction method. Raw powders of Pr_6O_{11} , Y_2O_3 , Co_3O_4 , and CaCO_3 were weighed with proper molar ratios and ground. Mixed powders were calcined at 1000 °C for 24 h in air. The calcined material was pulverized, ground, and pressed into a pellet 20 mm in diameter and 4 mm in thickness. The pellet was sintered at 1200 °C for 24 h under 1 bar of flowing oxygen gas. The powder X-ray diffraction pattern was taken at room temperature, in which a single-perovskite phase of orthorhombic symmetry with $Pbnm$ space group was confirmed. The measured density of the sample was above 90% from ideal. The rectangular shaped sample was prepared by cutting an as-sintered pellet. The electrical resistivity, $\rho(T)$, was measured in the temperature range 4–80 K by a dc four-probe method with a typical current density of 0.01 A/cm² under magnetic fields up to 17 T using the 20-T superconducting magnet (20 T-SM) at the HFL-SM, Tohoku University. The magnetic properties were investigated in the temperature range 2–300 K using DC superconducting quantum interference device (SQUID) magnetometer (MPMS XL, Quantum Design (QD)). The DC extraction magnetization up to 12 T was measured using an AC/DC magnetometer of the physical property measuring system (PPMS with the ACMS option, QD).

III. RESULTS AND DISCUSSION

The temperature dependence of the electrical resistivity, $\rho(T)$, for the $(\text{Pr}_{0.9375}\text{Y}_{0.0625})_{0.7}\text{Ca}_{0.3}\text{CoO}_3$ sample in various magnetic fields up to 17 T is presented in Figure 1. The absolute value of $\rho(T)$ is shown for zero magnetic field; the other curves are shifted appropriately for ease of viewing. To illustrate the thermal hysteresis, several modes of measurements were used. For zero magnetic field, $\rho(T)$ was measured in a run cycle commencing with cooling and subsequent heating. The results show that $\rho(T)$ moderately increases with decreasing temperature, undergoes an abrupt jump of about one order of magnitude at $T_{\text{MI-SS}} = 40$ K, and increases

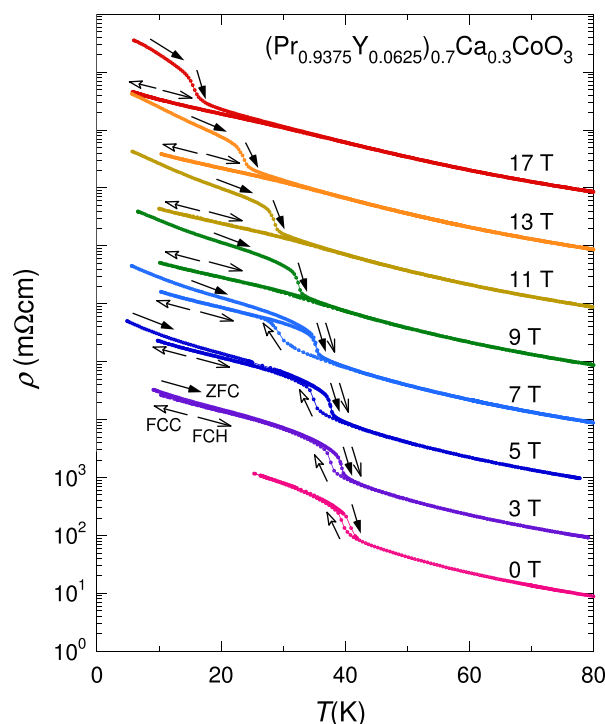


FIG. 1. Temperature dependence of the electrical resistivity, $\rho(T)$, of $(\text{Pr}_{0.9375}\text{Y}_{0.0625})_{0.7}\text{Ca}_{0.3}\text{CoO}_3$ sample in various magnetic fields up to $\mu_0 H = 17$ T. Measurements in each successive field are offset by an order of magnitude for clarity.

further as temperature decreases. In the subsequent heating, a similar sharp drop in $\rho(T)$ occurs but at the higher temperature of 41 K, a characteristic of hysteretic behavior for a first-order transition. We classify the $\rho(T)$ behavior above the transition temperature $T_{\text{MI-SS}}$ as metallic, as reported in previous papers.^{8,11}

In the presence of a magnetic field, $\rho(T)$ was measured for three different modes using both zero-field-cooled (ZFC) and field-cooled (FC) regimes as follows. First, after the sample was cooled to about 4.2 K in zero magnetic field, $\rho(T)$ was measured under an applied magnetic field during heating (ZFC). Thereafter, $\rho(T)$ was again measured while cooling (FCC) and subsequent heating (FCH) runs in the same applied magnetic field. In the ZFC mode, the MI-SS transition temperature $T_{\text{MI-SS}}(\text{ZFC})$ decreases gradually with increasing magnetic field, $\mu_0 H$, and the MI-SS transition survives up to 17 T. In contrast, in the FCC mode, the MI-SS transition occurs at a lower temperature $T_{\text{MI-SS}}(\text{FCC})$, which decreases more rapidly with increasing applied field, thus enhancing the hysteresis. The transition abruptly disappears at about 9 T. The subsequent FCH mode, with magnetic fields up to 7 T, the $T_{\text{MI-SS}}(\text{FCH})$ is nearly the same as $T_{\text{MI-SS}}(\text{ZFC})$. However, for magnetic fields above 9 T, the $\rho(T)$ behavior during FCH retraces that of the FCC run. The magnetic field dependence of $T_{\text{MI-SS}}$ is in clear contrast with the isostatic pressure dependence of $T_{\text{MI-SS}}$ in the $\text{Pr}_{1-x}\text{Ca}_x\text{CoO}_3$ samples,¹⁰ where $T_{\text{MI-SS}}$ increases with increasing pressure; sufficiently high pressures may induce a transition in the sample that is absent under ambient pressure.

Figure 2 presents the results of the magnetic field scans of electrical resistivity, $\rho(H)$, for $(\text{Pr}_{0.9375}\text{Y}_{0.0625})_{0.7}\text{Ca}_{0.3}\text{CoO}_3$ at several temperatures. In the ZFC mode, as shown in Fig. 2(a), the $\rho(H)$ at 4.2 K monotonically decreases (increases) with increasing (decreasing) applied magnetic field and only little irreversibility is observed. A similar behavior is found at 10 K but with a more pronounced irreversibility. At 20 K, the $\rho(H)$ shows a sudden drop at about 14.5 T in the ascending run, and abruptly increases at about 5.3 T in the descending run with a wide hysteresis of about 9 T. Similar hysteretic behaviors are observed at 30 K and 38 K. However, the width of the hysteresis and the transition temperature $T_{\text{MI-SS}}(H)$ decrease with increasing temperature. At 41.7 K, no hysteresis can be found again, because this temperature is just above the $T_{\text{MI-SS}}$ at $\mu_0 H = 0$ T and the system is in a metallic state. In the FC mode, i. e., after cooling the sample at 17 T, the $\rho(H)$ curves shown in Fig. 2(b), closely resemble those in the ZFC mode in Fig. 2(a), except that the transition magnetic field is slightly lower. The absolute value of $\rho(H)$ at 4.2 K is about one order of magnitude smaller than that of the ZFC mode, which confirms the metallic state and corroborates the idea that the MI-SS transition is suppressed at low temperatures above 9 T, as shown in Fig. 1.

Figure 3 depicts the temperature dependence of the molar magnetization, $M(T)$, for $(\text{Pr}_{0.9375}\text{Y}_{0.0625})_{0.7}\text{Ca}_{0.3}\text{CoO}_3$ in various magnetic fields, both in the ZFC and FCC modes. $M(T)$ at $\mu_0 H = 0.1$ T decreases with increasing temperature, jumps up at 41 K, and subsequently decreases with further increase in temperature. In the FCC mode, $M(T)$ nearly

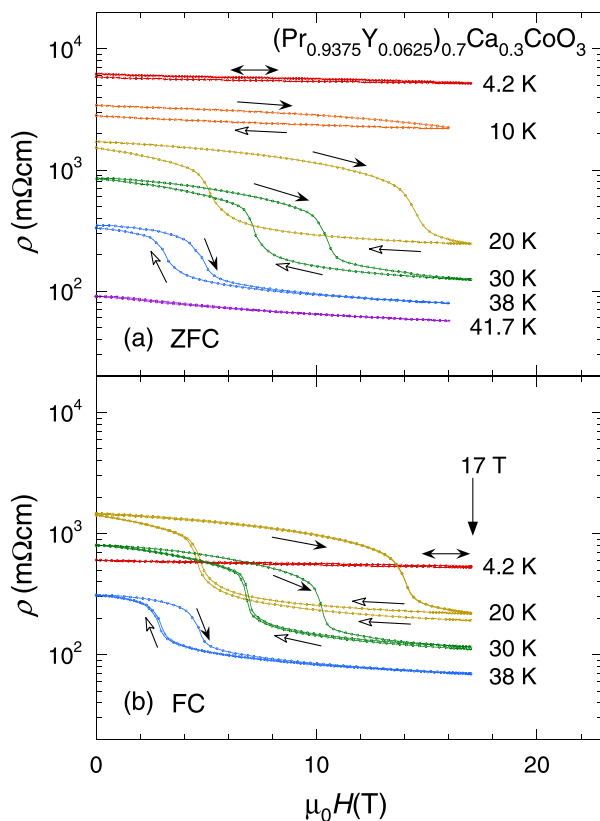


FIG. 2. Magnetic-field dependence of the electrical resistivity, $\rho(H)$, for $(\text{Pr}_{0.9375}\text{Y}_{0.0625})_{0.7}\text{Ca}_{0.3}\text{CoO}_3$ at various temperatures—during (a) the ZFC sample and (b) sample after FC at 17 T.

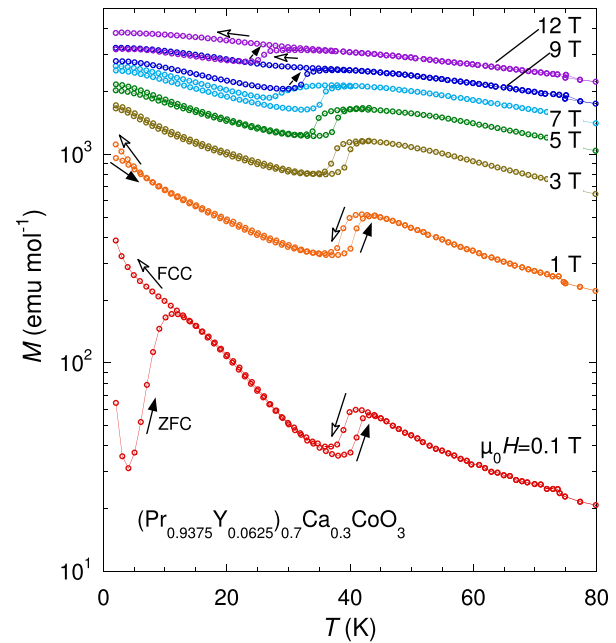


FIG. 3. Temperature dependence of the molar magnetization, $M(T)$, of $(\text{Pr}_{0.9375}\text{Y}_{0.0625})_{0.7}\text{Ca}_{0.3}\text{CoO}_3$ in various magnetic fields. The ZFC/FCC bifurcation, seen for the lowest field at 12 K, points to an existence of minor (yttrium poorer) regions that do not undergo the MI transition and develop ferromagnetic clusters at a lower temperature.

retraces the curve of the ZFC mode, but the transition during the cooling run occurs at a lower temperature of 39 K, thus producing hysteresis. The behavior in the $M(T)$ curves at magnetic fields below $\mu_0 H = 5$ T is quite similar to that at $\mu_0 H = 0.1$ T, but the transition temperature decreases with increasing magnetic field. However, the transition in the FCC mode broadens at 7 T, and widens out at magnetic fields above 9 T. The magnetic response is consistent with the $\rho(T)$ curves shown in Fig. 1.

Similar to the previously studied compounds with higher yttrium content ($y = 0.075 - 0.15$, $T_{\text{MI-SS}} = 64 - 132$ K),¹⁵ the transition in $y = 0.0625$ is associated with a crossover of cobalt ions to a low-spin ground state that is promoted by a significant shift in the mixed-valence $\text{Co}^{3+}/\text{Co}^{4+}$ toward the pure Co^{3+} . This process is compensated by the valence change of some Pr^{3+} ions to Pr^{4+} ions;^{13,15} we determined the final amount to be 0.11 Pr^{4+} per f. u. based on the Schottky peak in heat capacity under ZFC (experiment to be published elsewhere). Surprisingly, we detected a certain reduced amount of Pr^{4+} even after a cooling run in a 9-T field, when the MI-SS transition was suppressed and the $y = 0.0625$ sample remained in the metallic state. We note that the jumps in electrical resistivity and magnetization actually observed do not represent the whole crossover as the phase evolution is not confined solely to temperatures near $T_{\text{MI-SS}}$; see, e. g., the smooth temperature dependence of the x-ray absorption near-edge structure (XANES) data at the Pr- L_3 edge for both the $\text{Pr}_{0.5}\text{Ca}_{0.5}\text{CoO}_3$ and $(\text{Pr}_{1-y}\text{Y}_y)_{0.7}\text{Ca}_{0.3}\text{CoO}_3$.^{12,15} To explain this behaviour, we may refer to a model of the LS/HS crossover in a mean field approximation, presented in Ref. 22. It is shown that the crossover generally proceeds in a gradual way as local excitations, but in the presence of strong inter-correlations it may acquire the characteristics of a phase

transition as found for the present cobaltite. In these model simulations, three stages have been identified. First, HS states are locally excited and their equilibrium population slowly increases with increasing temperature. Then, the HS concentration undergoes a sudden jump. After this, there is again a smooth increase up to a high-temperature saturation of the HS/LS ratio.

The transition temperature $T_{\text{MI-SS}}$ as a function of the magnetic field for the $(\text{Pr}_{0.09375}\text{Y}_{0.0625})_{0.7}\text{Ca}_{0.3}\text{CoO}_3$ sample is shown in Figure 4, which was plotted based on the resistivity and magnetization data in Figs. 1 and 3. The $T_{\text{MI-SS}}$ values determined from $M(T)$ almost coincide with those determined from $\rho(T)$, which suggests that the MI and SS transitions remain coupled for all applied fields, and has thus a common microscopic origin. This is obviously resulting from the stabilization of the IS-Co^{3+} state by the magnetic field because of its larger spin, which affects the thermally driven transition from the low-temperature LS-Co^{3+} dominant phase to the metallic phase of mixed $\text{IS-Co}^{3+}/\text{LS-Co}^{4+}$ character. The formula for the shift in the transition temperature with magnetic field can be deduced from general thermodynamic relations (see, e. g., Refs. 21 and 22),

$$T_{\text{MI-SS}}(\mu_0 H) = T_{\text{MI-SS}}(0) - A(\mu_0 H)^2, \quad (1)$$

where $T_{\text{MI-SS}}(0)$ is the transition temperature at zero field and $A = \Delta\chi/(2\Delta S)$ is a parameter that is physically related to the change in magnetic susceptibility $\Delta\chi$ and the change in entropy ΔS during the first-order transition. Using this equation and A as a fitting parameter, the experimentally obtained results are well reproduced. The fits for the ZFC and FCC runs are shown by the broken lines in Fig. 4, corresponding to $A = 0.09 \text{ K T}^{-2}$ and 0.2 K T^{-2} , respectively. The results suggest that the MI-SS transition in the ZFC mode disappears approximately at 21 T, i.e., not far above our experimental range. However, the MI-SS transition in the FCC mode is observed to be abruptly suppressed in a 9-T magnetic field, although the MI-SS transition line

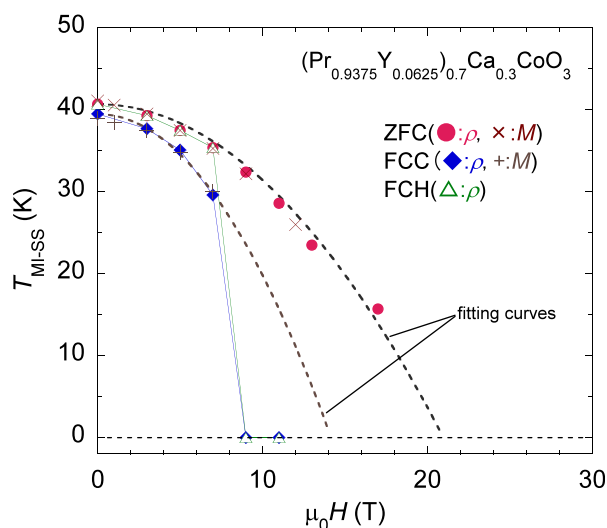


FIG. 4. Phase diagram of the $(\text{Pr}_{0.09375}\text{Y}_{0.0625})_{0.7}\text{Ca}_{0.3}\text{CoO}_3$ sample in the (H, T) plane. Dashed lines represent fitted curves for the transition temperature, $T_{\text{MI-SS}}(\mu_0 H)$, using Eq. (1).

extrapolates to zero at 14 T. Based on the above mentioned value $A = 0.09 \text{ K T}^{-2}$ and the susceptibility change deduced for the $y = 0.0625$ sample from Fig. 3, $\Delta\chi = 0.02 \text{ emu mol}^{-1} \text{Oe}^{-1}$, we estimate the entropy change during the thermally induced transition to be $\Delta S = 1.1 \text{ J mol}^{-1} \text{K}^{-1}$. Using the same approach, $\Delta S = 3.2 \text{ J mol}^{-1} \text{K}^{-1}$ was obtained previously for a sample with higher yttrium content, $y = 0.075$.²¹ These ΔS values are significantly larger than the total entropy change obtained from heat capacity measurements, $0.28 \text{ J mol}^{-1} \text{K}^{-1}$ and $2.2 \text{ J mol}^{-1} \text{K}^{-1}$ for $y = 0.0625$ and 0.075 , respectively. This discrepancy suggests that the magnetic part of the entropy change will be partially compensated by other terms.

In summary, the $(\text{Pr}_{1-y}\text{Y}_y)_{0.7}\text{Ca}_{0.3}\text{CoO}_3$ compound ($y = 0.0625$, $T_{\text{MI-SS}} = 40 \text{ K}$), situated at the lower limit for the occurrence of the first-order MI and SS transitions, has been studied using electrical resistivity and magnetization measurements in magnetic fields up to 17 T. The experimental data suggest that the energy difference between the LS and IS states of Co^{3+} and Co^{4+} ions is fairly small and becomes comparable with the energy scale of commonly accessible magnetic fields. Thus, the MI-SS transition can be driven both thermally and magnetically, resulting in a complex phase diagram in the (H, T) plane with important hysteretic behaviors. The detailed mechanism for the MI-SS transition in the system, as well as the role of $\text{Pr}^{3+} \rightarrow \text{Pr}^{4+}$ valence shift still needs to be clarified.

ACKNOWLEDGMENTS

This work was partly supported by JSPS KAKENHI Grant No. 24540355. The experiments in Institute of Physics Prague were supported by Project No. 13-03708S of the Grant Agency of the Czech Republic.

- ¹P. M. Raccah and J. B. Goodenough, *Phys. Rev.* **155**, 932 (1967).
- ²M. A. Korotin, S. Yu. Ezhov, I. V. Solov'yev, V. I. Anisimov, D. I. Khomskii, and G. A. Sawatzky, *Phys. Rev. B* **54**, 5309 (1996).
- ³S. Medling, Y. Lee, H. Zheng, J. F. Mitchell, J. W. Freeland, B. N. Harmon, and F. Bridges, *Phys. Rev. Lett.* **109**, 157204 (2012).
- ⁴P. Augustinsky, V. Krapek, and J. Kunes, *Phys. Rev. Lett.* **110**, 267204 (2013).
- ⁵A. O. Sboychakov, K. I. Kugel, A. L. Rakhmanov, and D. I. Khomskii, *Phys. Rev. B* **80**, 024423 (2009).
- ⁶J. Wu and C. Leighton, *Phys. Rev. B* **67**, 174408 (2003).
- ⁷Z. Jiráček, J. Hejtmánek, K. Knížek, M. Maryško, P. Novák, E. Šantavá, T. Naito, and H. Fujishiro, *J. Phys.: Condens. Matter* **25**, 216006 (2013).
- ⁸S. Tsubouchi, T. Kyōmen, M. Itoh, P. Ganguly, M. Oguni, Y. Shimojo, Y. Morii, and Y. Ishii, *Phys. Rev. B* **66**, 052418 (2002).
- ⁹S. Tsubouchi, T. Kyōmen, M. Itoh, and M. Oguni, *Phys. Rev. B* **69**, 144406 (2004).
- ¹⁰T. Fujita, T. Miyashita, Y. Yasui, Y. Kobayashi, M. Sato, E. Nishibori, M. Sakata, Y. Shimojo, N. Igawa, Y. Ishii, K. Kakurai, T. Adachi, Y. Ohishi, and M. Takata, *J. Phys. Soc. Jpn.* **73**, 1987 (2004).
- ¹¹T. Naito, H. Sasaki, and H. Fujishiro, *J. Phys. Soc. Jpn.* **79**, 034710 (2010).
- ¹²J. Hejtmánek, Z. Jiráček, O. Kaman, K. Knížek, E. Šantavá, K. Nitta, T. Naito, and H. Fujishiro, *Eur. Phys. J. B* **86**, 305 (2013).
- ¹³J. L. García-Muñoz, C. Frontera, A. J. Barón-González, S. Valencia, J. Blasco, R. Feyerherm, E. Dudzik, R. Abrudan, and F. Radu, *Phys. Rev. B* **84**, 045104 (2011).
- ¹⁴J. Hejtmánek, E. Šantavá, K. Knížek, M. Maryško, Z. Jiráček, T. Naito, H. Sasaki, and H. Fujishiro, *Phys. Rev. B* **82**, 165107 (2010).
- ¹⁵H. Fujishiro, T. Naito, S. Ogawa, N. Yoshida, K. Nitta, J. Hejtmánek, K. Knížek, and Z. Jiráček, *J. Phys. Soc. Jpn.* **81**, 064709 (2012).

- ¹⁶K. Knížek, J. Hejtmánek, M. Maryško, P. Novák, E. Šantavá, Z. Jiráček, T. Naito, H. Fujishiro, and Clarina de la Cruz, *Phys. Rev. B* **88**, 224412 (2013).
- ¹⁷F. Guillou, Q. Zhang, Z. Hu, C. Y. Kuo, Y. Y. Chin, H. J. Lin, C. T. Chen, A. Tanaka, L. H. Tjeng, and V. Hardy, *Phys. Rev. B* **87**, 115114 (2013).
- ¹⁸H. Fujishiro, T. Naito, D. Takeda, N. Yoshida, T. Watanabe, K. Nitta, J. Hejtmánek, K. Knížek, and Z. Jiráček, *Phys. Rev. B* **87**, 155153 (2013).
- ¹⁹Y. Qi, E. W. Müller, H. Spiering, and P. Gülich, *Chem. Phys. Lett.* **101**, 503 (1983).
- ²⁰Y. Ogawa, T. Ishikawa, S. Koshihara, K. Boukheddaden, and F. Varret, *Phys. Rev. B* **66**, 073104 (2002).
- ²¹M. Maryško, Z. Jiráček, K. Knížek, P. Novák, J. Hejtmánek, T. Naito, H. Sasaki, and H. Fujishiro, *J. Appl. Phys.* **109**, 07E127 (2011).
- ²²Y. Garcia, O. Kahn, J.-P. Ader, A. Buzdin, Y. Meurdesoif, and M. Guillot, *Phys. Lett. A* **271**, 145 (2000).